

CoIO-RAN: Developing Machine Learning-based xApps for Open RAN Closed-loop Control on Programmable Experimental Platforms

Michele Polese, *Member, IEEE*, Leonardo Bonati, *Student Member, IEEE*,
Salvatore D'Oro, *Member, IEEE*, Stefano Basagni, *Senior Member, IEEE*,
Tommaso Melodia, *Fellow, IEEE*



Abstract—Cellular networks are undergoing a radical transformation toward disaggregated, fully virtualized, and programmable architectures with increasingly heterogeneous devices and applications. In this context, the open architecture standardized by the O-RAN Alliance enables algorithmic and hardware-independent Radio Access Network (RAN) adaptation through closed-loop control. O-RAN introduces Machine Learning (ML)-based network control and automation algorithms as so-called *xApps* running on RAN Intelligent Controllers. However, in spite of the new opportunities brought about by the Open RAN, advances in ML-based network automation have been slow, mainly because of the unavailability of large-scale datasets and experimental testing infrastructure. This slows down the development and widespread adoption of Deep Reinforcement Learning (DRL) agents on real networks, delaying progress in intelligent and autonomous RAN control. In this paper, we address these challenges by proposing practical solutions and software pipelines for the design, training, testing, and experimental evaluation of DRL-based closed-loop control in the Open RAN. We introduce CoIO-RAN, the first publicly-available large-scale O-RAN testing framework with software-defined radios-in-the-loop. Building on the scale and computational capabilities of the Colosseum wireless network emulator, CoIO-RAN enables ML research at scale using O-RAN components, programmable base stations, and a “wireless data factory”. Specifically, we design and develop three exemplary *xApps* for DRL-based control of RAN slicing, scheduling and online model training, and evaluate their performance on a cellular network with 7 softwarized base stations and 42 users. Finally, we showcase the portability of CoIO-RAN to different platforms by deploying it on Arena, an indoor programmable testbed. Extensive results from our first-of-its-kind large-scale evaluation highlight the benefits and challenges of DRL-based adaptive control. They also provide insights on the development of wireless DRL pipelines, from data analysis to the design of DRL agents, and on the tradeoffs associated to training on a live RAN. CoIO-RAN and the collected large-scale dataset will be made publicly available to the research community.

Index Terms—O-RAN, Network Intelligence, 5G/6G, Deep Reinforcement Learning, Colosseum

The authors are with the Institute for the Wireless Internet of Things, Northeastern University, Boston, MA, USA. E-mail: {m.polese, l.bonati, s.doro, s.basagni, t.melodia}@northeastern.edu.

This work was partially supported by the U.S. National Science Foundation under Grants CNS-1923789, CNS-1925601, CNS-2120447, and CNS-2112471, and the U.S. Office of Naval Research under Grant N00014-20-1-2132.

1 INTRODUCTION

In addition to providing traditional voice and data connectivity services, cellular systems are becoming increasingly pervasive in industrial and agricultural automation, interconnecting millions of sensors, vehicles, airplanes, and drones, and providing the nervous system for a plethora of smart systems [1, 2]. These diverse use cases, however, often come with heterogeneous—possibly orthogonal—network constraints and requirements [3]. For instance, autonomous driving applications require Ultra Reliable and Low Latency Communications (URLLC) to allow vehicles to promptly react to sudden events and changing traffic conditions. Instead, high-quality multimedia content requires high data rates, but can tolerate a higher packet loss and latency. Therefore, the future generations of cellular networks need to be *flexible* and *adaptive* to many different application and user requirements.

To achieve these goals, future Radio Access Networks (RANs) will need to combine three key ingredients [4]: (i) *programmable and virtualized protocol stacks* with clearly defined, open interfaces; (ii) *closed-loop network control*, and (iii) *data-driven modeling and Machine Learning (ML)*. Programmability will allow swift adaptation of the RAN to provide bespoke services able to satisfy the requirements of specific deployments. Closed-loop control will leverage telemetry measurements from the RAN to reconfigure cellular nodes, adapting their behavior to current network conditions and traffic. Last, data-driven modeling will exploit recent developments in ML and big data to enable real-time, closed-loop, and dynamic decision-making based, for instance, on Deep Reinforcement Learning (DRL) [5]. These are the very same principles at the core of the Open RAN paradigm, which has recently gained traction as a practical enabler of algorithmic and hardware innovation in future cellular networks [6–8].

To promote the evolution toward open RAN architectures, 3GPP has standardized disaggregated base stations that are split into a number of different functional units, the Central Unit (CU), Distributed Unit (DU), and Radio Unit (RU). The O-RAN Alliance, an industry consortium,

is standardizing open interfaces that connect the various disaggregated functional units to a common control overlay, the RAN Intelligent Controller (RIC), capable of executing custom control logic via so-called *xApps*. Ultimately, these efforts will render the *monolithic RAN "black-box"* obsolete, favoring *open, programmable and virtualized* solutions that expose status and offer control knobs through standardized interfaces [4].

Intelligent, dynamic network optimization via add-on software *xApps* is clearly a key enabler for future network automation. However, it also introduces novel practical challenges concerning, for instance, the deployment of data-driven ML control solutions at scale. Domain-specific challenges stem from considering the constraints of standardized RANs, the very nature of the wireless ecosystem and the complex interplay among different elements of the networking stack. These challenges, all yet to be addressed in practical RAN deployments, include:

- 1) *Collecting datasets at scale.* Datasets for ML training/testing at scale need to be carefully collected and curated to accurately represent the intrinsic randomness and behavior of real-world RANs.
- 2) *Testing ML-based control at scale.* Even if ML algorithms are trained on properly collected data, it is necessary to assess their robustness at scale, especially when considering closed-loop control, to prevent poorly-designed data-driven solutions from causing outages or sub-optimal performance.
- 3) *Designing efficient ML agents with unreliable input and constrained output.* In production systems, real-time collection of data from the RAN may be inconsistent (e.g., with varying periodicity) or incomplete (e.g., missing entries), and control actions may be constrained by standard specification.
- 4) *Designing ML agents capable of generalizing.* Agents should be able to generalize and adapt to unseen deployment configurations not part of the training set.
- 5) *Selecting meaningful features.* Features should be accurately selected to provide a meaningful representation of the network status without incurring into dimensionality issues.

Contributions. To address these key challenges, in this paper we describe the design of DRL-based *xApps* for closed-loop control in O-RAN and their testing in a first-of-its-kind softwarized pipeline on large-scale experimental platforms. Based on this experience, we review and discuss key insights in the domain of ML design for O-RAN networks. Notably, our contributions are as follows:

- We introduce CoIO-RAN, a first-of-its-kind open, large-scale, experimental O-RAN framework for training and testing ML solutions for next-generation RANs. It combines O-RAN components, a softwarized RAN framework [9], and Colosseum, the world’s largest, open, and publicly-available wireless network emulator based on Software-defined Radios (SDRs) [10]. Specifically, CoIO-RAN leverages Colosseum as a *wireless data factory* to generate large-scale datasets for ML training in a variety of Radio Frequency (RF) environments, taking into account propagation and fading characteristics of real-world deployments. The ML models are deployed as *xApps* on the near-real-time RIC, which connects to RAN nodes through O-RAN-compliant interfaces for data collection and closed-loop control. CoIO-RAN is the first platform that enables wireless researchers to deploy ML

solutions on a full-stack, fully virtualized O-RAN environment which integrates large-scale data collection and DRL testing capabilities with SDRs. Moreover, CoIO-RAN also offers a lightweight, containerized implementation that can be easily ported to other experimental platforms. *CoIO-RAN and the dataset created for this paper will be open-sourced and made publicly available to the research community.*

- We develop three *xApps* for closed-loop control of RAN scheduling and slicing policies, and for the online training of DRL agents on live production environments. We propose an innovative *xApp* design based on the combination of an autoencoder with the DRL agent to improve the resilience and robustness to real, imperfect network telemetry. We then utilize CoIO-RAN to provide insights on the performance of the DRL agents for adaptive RAN control at scale. We train the autoencoders and agents over a 3.4 GB dataset with more than 73 hours of live RAN performance traces, and perform one of the first evaluations of DRL agents autonomously driving a programmable, software-defined RAN with 49 nodes. Lessons learned from this evaluation span from the design to the deployment of DRL agents for RAN control. They include new understandings of data analysis and feature selection, modeling of control actions for DRL agents, and design strategies to train ML algorithms that generalize and operate even with unreliable data.
- We analyze the tradeoffs of training of DRL agents on live networks using Colosseum and Arena (a publicly-available indoor testbed for spectrum research [11]) with commercial smartphones. We profile the RAN performance during the DRL exploration phase and after the training, showing how an extra online training step adapts a pre-trained model to deployment-specific parameters, fine-tuning its weights at the cost of a temporary performance degradation in the online exploration phase.

Key takeaways from our work highlight (i) the effectiveness of adaptive control policies over static configurations, even if the latter are optimized; (ii) the impact of different design choices of DRL agents on end-to-end network performance, and (iii) the importance of online DRL training in wireless environments. We believe that these insights and the research infrastructure developed in this work can catalyze, promote and further the deployment of ML-enabled control loops in next generation networks.

The rest of this paper is organized as follows. Section 2 describes the development of ML solutions in O-RAN-based networks. Section 3 introduces CoIO-RAN, and Section 4 presents the *xApp*, DRL agent design, and the data collection campaign for offline training. Large-scale evaluation and lessons learned are discussed in Sections 5 and 6. Section 7 reviews related work. Finally, Section 8 concludes the paper.

2 MACHINE LEARNING FOR THE OPEN RAN

The deployment of machine learning models in wireless networks is a multi-step process (Fig. 1). It involves a data collection step, the design of the model, its offline or online training and deployment for runtime inference and control. The O-RAN architecture, also shown in Fig. 1, has been developed to aid the overall deployment process, focusing

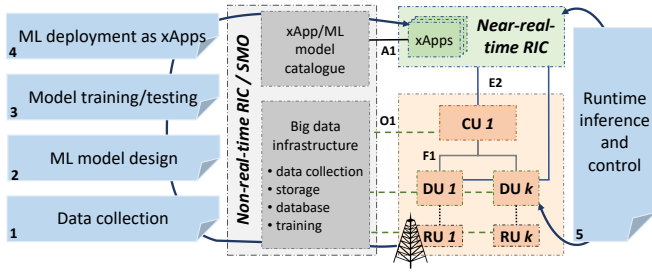


Fig. 1: The O-RAN architecture and the workflow for the design, development and deployment of ML applications in next generation wireless networks.

on open interfaces for data collection and deployment steps. In the following, we describe the O-RAN architecture, and discuss how it facilitates training and deploying ML models in the RAN.

2.1 O-RAN Overview

The O-RAN Alliance, a consortium of academic and industry members, has been pushing forward the concept of an open and programmable cellular ecosystem since its inception in 2018. O-RAN-compliant equipment is based on open and standardized interfaces that enable interoperability of equipment from different vendors and interaction with RAN controllers, which manage the RAN itself. The O-RAN specifications introduce two RICs that perform network control procedures over different time scales, i.e., *near-real-time* and *non-real-time*, respectively [12]. The non-real-time RIC performs operations at time scales larger than 1 s and can involve thousands of devices. Examples include Service Management and Orchestration (SMO), policy management, training and deployment of ML models. The near-real-time RIC, instead, implements tight control loops that span from 10 ms to 1 s, involving hundreds of CUs/DUs. Procedures for load balancing, handover, RAN slicing policies [13] and scheduler configuration are examples of near-real-time RIC operations [14]. The near-real-time RIC can also hosts third-party applications, i.e., *xApps*. *xApps* implement control logic through heuristics or data-driven control loops, as well as collect and analyze data from the RAN.

The components of the O-RAN architecture are connected via open and standardized interfaces. The non-real-time RIC uses the O1 interface to collect data in bulk from RAN nodes and to provision services and network functions. The near-real-time RIC connects to CUs and DUs through the E2 interface, which supports different Service Models (SMs), i.e., functionalities like reporting of Key Performance Measurements (KPMs) from RAN nodes and the control of their parameters [15]. The two RICs connect through the A1 interface for the deployment of policies and *xApps* on the near-real-time RIC.

2.2 ML Pipelines in O-RAN

The O-RAN specifications include guidelines for the management of ML models in cellular networks. Use cases and applications include Quality of Service (QoS) optimization and prediction, traffic steering, handover, and radio fingerprinting [5]. The specifications describe the ML workflow

for O-RAN through five steps (Fig. 1): (1) data collection; (2) model design; (3) model training and testing; (4) model deployment as *xApp*, and (5) runtime inference and control.

First, data is collected for different configurations and setups of the RAN (e.g., large/small scale, different traffic, step 1). Data is generated by the RAN nodes, i.e., CUs, DUs and RUs, and streamed to the non-real-time RIC through the O1 interface, where it is organized in large datasets. After enough data has been collected, an ML model is designed (step 2). This entails the following: (i) identifying the RAN parameters to input to the model (e.g., throughput, latency, etc.); (ii) identifying the RAN parameters to control as output (e.g., RAN slicing and scheduling policies), and (iii) the actual ML algorithm implementation. Once the model has been designed and implemented, it is trained and tested on the collected data (step 3). This involves selecting the model hyperparameters (e.g., the depth and number of layers of the neural network) and training the model on a portion of the collected data until a (satisfactory) level of convergence of the model has been reached. After the model has been trained, it is tested on an unseen portion of the collected data to verify that it is able to generalize and react to potentially unforeseen situations. Then, the model is packaged into an *xApp* ready to run on the near-real-time RIC (step 4). After the *xApp* has been created, it is deployed on the O-RAN infrastructure. In this phase, the model is first stored in the *xApp* catalogue of the non-real-time RIC, and then instantiated on demand on the near-real-time RIC, where it is interfaced with the RAN through the E2 interface to perform runtime inference and control based on the current network conditions (step 5).

3 COLO-RAN: ENABLING LARGE-SCALE ML RESEARCH WITH O-RAN AND COLOSSEUM

The ML pipeline described in Section 2.2 involves a number of critical steps whose execution requires joint access to *comprehensive datasets* and *testing facilities at scale*, still largely unavailable to the research community. In fact, even major telecom operators or infrastructure owners might not be able to dedicate (parts of) their extensive commercial networks to training and testing of ML algorithms. This stems from the lack of adequate solutions to separate testing from commercial service and to prevent performance degradation. As a consequence, researchers and innovators are constrained to work with small ad hoc datasets collected in contained lab setups, resulting in solutions that hardly generalize to real-world deployments [16].

To address this limitation, this section introduces CoLo-RAN, a large-scale research infrastructure built upon the Colosseum network emulator to train, deploy, and test state-of-the-art wireless ML solutions. We first review the main features of Colosseum and describe its use as a wireless data factory for CoLo-RAN (Section 3.1). Then, we introduce the implementation of the CoLo-RAN virtualized O-RAN infrastructure on Colosseum (Section 3.2) and of the *xApps* we designed (Section 4). We finally describe the scenario for data collection that we use to illustrate the usage of CoLo-RAN (Section 4.3).

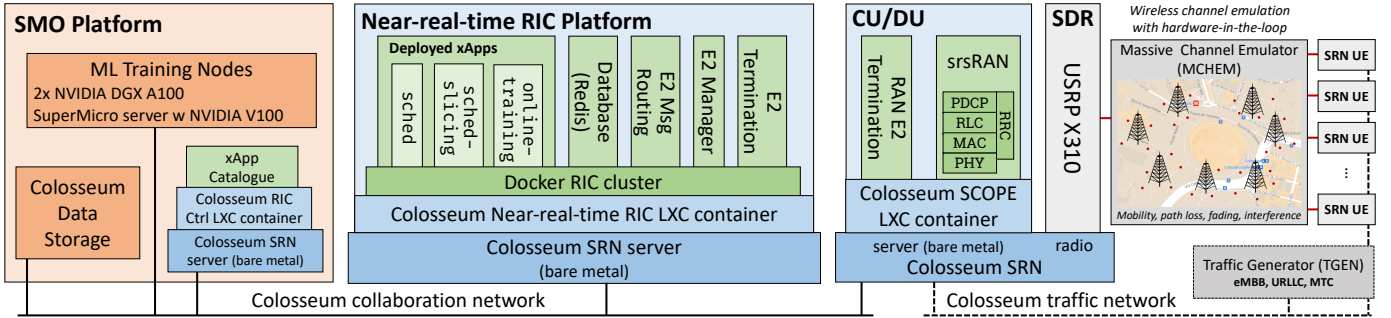


Fig. 2: Integration of the O-RAN infrastructure in Colosseum.

3.1 Colosseum as a Wireless Data Factory

Colosseum is the world’s largest wireless network emulator [10]. It was developed by DARPA for the Spectrum Collaboration Challenge and then transitioned to the U.S. National Science Foundation PAWR program to be available for the research community. Colosseum includes 256 USRP X310 SDRs. Half of the SDRs can be controlled by the users, while the other half is part of the Massive Channel Emulator (MChem), which uses 64 Virtex-7 FPGAs to emulate wireless channels. MChem processes the signals transmitted by radio nodes—called Standard Radio Nodes (SRNs) in Colosseum—through a set of complex-valued finite impulse response filter banks. These model propagation characteristics and multi-path scattering of user-defined wireless environments, as shown in the right part of Fig. 2. Thus, MChem provides high-fidelity emulation of wireless signals with the same characteristics of those traveling through a real environment. Colosseum also features a user-controlled source Traffic Generator (TGEN), based on MGEN [17], and compute capabilities that make it a full-fledged specialized data center with over 170 high-performance servers.

The combination of programmable software-defined hardware with RF and traffic scenarios uniquely positions Colosseum as a wireless data factory, namely, as a tool that can be used to effectively collect full-stack datasets in heterogeneous and diverse scenarios. With respect to other large testbeds such as the PAWR platforms, Colosseum offers scale and a more controlled and customizable environment that researchers can use to collect data and to test ML algorithms on different RF scenarios and frequencies, without changing the protocol stack or experimental procedures. Compared to a production network, Colosseum is flexible, with programmable radios that can run different software-defined stacks, and the possibility to test closed-loop control without affecting commercial deployments.

3.2 O-RAN-based Colosseum ML Infrastructure

Besides enabling large-scale data collection, Colosseum also provides a hybrid RF and compute environment for the deployment of CoO-RAN, a complete end-to-end ML infrastructure. CoO-RAN provides researchers with a ready-to-use environment to develop and test ML solutions, following the steps of Fig. 1 (Section 2.2). These include the deployment on a 3GPP-compliant RAN, testing in heterogeneous emulated environments, and an O-RAN-compliant

infrastructure. With respect to other open source implementations of the O-RAN infrastructure, CoO-RAN features a more lightweight footprint (e.g., it does not require a full Kubernetes deployment, contrary to the O-RAN Software Community (OSC) RIC), and it can be ported to other testbeds, e.g., Arena [11], with minimal changes, thanks to its virtualized and container-based implementation. As a further contribution, this platform will be made openly available to the research community upon acceptance of this paper.

The software, compute and networking components of our end-to-end infrastructure are shown in Fig. 2. The SMO (left) features three compute nodes to train large ML models, 64 Terabyte of storage for models and datasets, and the xApp catalogue. The near-real-time RIC (Fig. 2, center) provides E2 connectivity to the RAN and support for multiple xApps interacting with the base stations. It is implemented as a standalone Linux Container (LXC) that can be deployed on a Colosseum SRN. It includes multiple Docker containers for the *E2 termination* and *manager*, the *E2 message routing* to handle messages internal to the RIC, a *Redis database*, which keeps a record of the nodes connected to the RIC, and the *xApps* (Section 4). The implementation of the near-real-time RIC is based on the Bronze release of the OSC [18]. The OSC near-real-time RIC was adapted into a minimal version, which does not require a Kubernetes cluster, and can fit in a lightweight LXC container. We also extended the OSC codebase to support concurrent connections from multiple base stations and xApps, and to provide improved support for encoding, decoding and routing of control messages.

The near-real-time RIC connects to the RAN base stations through the E2 interface (Fig. 2, right). The base stations leverage a joint implementation of the 3GPP DUs and CUs. These nodes run the publicly available SCOPE framework [9], which extends srsRAN [19] with open interfaces for runtime reconfiguration of base station parameters and automatic collection of relevant KPMs. Moreover, we leverage and extend the E2 termination of the OSC DU [20] to reconfigure the base stations directly from the near-real-time RIC and for periodic data reporting. The E2 termination allows the setup procedure and registration of the base stations with the near-real-time RIC. Our implementation also features two custom SMs (as discussed next) for trigger-based or periodic reporting, and control events in the base stations. This effectively enables data-driven real-time control loops between the base stations and the xApps. The RAN supports network slicing with 3 slices for different

QoS: (i) Enhanced Mobile Broadband (eMBB), representing users requesting video traffic; (ii) Machine-type Communications (MTC) for sensing applications, and (iii) URLLC for latency-constrained applications. Slicing is implemented in the SCOPE framework by applying Physical Resource Block (PRB) masks during the scheduling process, and it is possible to control the number of PRBs for each slice [9]. For each slice, the base stations can adopt 3 different scheduling policies independently of that of the other slices, namely, the Round Robin (RR), the Waterfilling (WF), and the Proportional Fair (PF) scheduling policies. These policies were selected as they represent popular scheduling strategies in wireless deployments [21]. Finally, the base stations connect to the RF frontends (USRP's X310) that perform signal transmission and reception.

4 xAPP DESIGN FOR DRL-BASED CONTROL

The xApps deployed on the near-real-time RIC are the heart of the O-RAN-based RAN control loops. We developed three xApps to evaluate the impact of different ML strategies for closed-loop RAN control (Table 1). Each xApp can receive data and control RAN nodes with two custom SMs, which resemble the O-RAN KPM and RAN control SMs [15]. The control actions available to the xApps are the selection of the slicing policy (the number of PRB allocated to each slice) and of the scheduling policy (which scheduler is used for each slice).

The xApps have been developed by extending the OSC basic xApp framework [22], and include two components (Fig. 3).

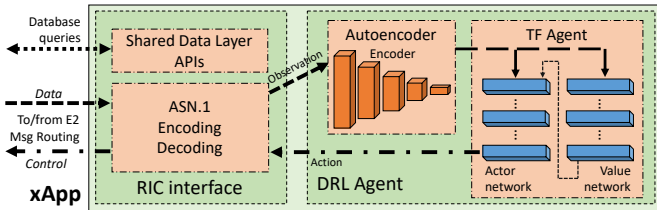


Fig. 3: Structure of a CoLo-RAN xApp.

The first is the interface to the RIC, which implements the SM and performs ASN.1 encoding/decoding of RAN data and control. The second is the ML infrastructure itself, which includes one or more autoencoders and DRL agents. For these, we used TensorFlow 2.4 [23] and the TF-Agents library [24].

4.1 DRL agent design

The DRL agents considered in this paper have been trained using the Proximal Policy Optimization (PPO) algorithm [25]. PPO is a well-established on-policy DRL architecture that uses an actor-critic configuration where the *actor* network takes actions according to current network state, and the value network (or *critic*) scores the actions taken by the actor network by observing the reward obtained when taking an action in a specific state of the environment. By leveraging this architecture, the PPO algorithm decouples the action taking process from the evaluation of achieved rewards. This is extremely important to ensure that the

actor network can learn an unbiased policy (i.e., a mapping between state and actions) where the actor network selects an action because it is effective in the long run and not only because it occasionally results in high instantaneous rewards that are instead inefficient in the majority of cases.

It is also worth mentioning that the actor-critic setup is also important because PPO is an on-policy architecture, which means that the training procedure uses a memory buffer that contains data that is collected by using actions that are taken with the most current version of the actor network. If compared to off-policy algorithms (such as Deep Q-Networks (DQNs)), which use a memory buffer that store experience collected at any time by the DRL agent, PPO only uses data that is fresh and not contain experiences from the past, meaning that the memory buffer is emptied every time the actor network is updated during the training phase. This approach is usually slower than other solutions, but together with the actor-critic setup it has been demonstrated as one of the most efficient and reliable DRL architectures in the literature [25].

Observations, Actions and Rewards. One of the main causes of slow training of DRL agents is the use of observations with high dimensionality that result in actor and critic networks with many parameters and large state space. Indeed, the RAN produces an extremely large amount of data which not always provide meaningful insights on the actual state of the system due to redundant information and outliers. To reduce the size of the observation fed to the DRL agent, mitigate outliers and provide a high-quality yet high-level representation of the state of the system, we resort to autoencoders, as also shown in Fig. 3. Specifically, before being fed to the DRL agents, the data produced by the RAN is processed by the encoding portion of an autoencoder for dimensionality reduction (whose impact on DRL-based control is investigated in Section 5.2).

Although autoencoders might have several implementations according to the specific applications, autoencoders for dimensionality reduction have an hourglass architecture with an encoder and a decoder components. The former produces a lower dimension representation of the input data (i.e., latent representation) which - if trained properly - can be accurately reconstructed by the decoder portion of the autoencoder with negligible error. The decoder is the specular image of the encoder and the goal of this architecture is to create a reduced version of the input data that contains only relevant information, yet it is accurate enough to be able to reconstruct the original data without any loss. To further reduce the complexity of the DRL agents, we perform feature selection on the metrics that are observed by the agents (see Section 5 for more details).

As mentioned before, each xApp embeds different DRL agents according to the specific goal of the xApp. For this reason, we have designed a set of DRL agents that observe different metrics of the RAN, take diverse actions and aim at maximizing different rewards. The configurations considered in this paper are shown in Table 1. The DRL agent of `sched-slicing` jointly selects the slicing and scheduling policy for a single base station and all slices. For this xApp we trained three DRL models: baseline (DRL-base), an agent that explores a reduced set of actions (DRL-reduced-actions) and an agent where input data is fed directly to

xApp	Functionality	Input (Observation)	Output (Action)	ML Models	Utility (Reward)
sched-slicing	Single-DRL-agent for joint slicing and scheduling control	Rate, buffer size, PHY TBs (DL)	PRB and scheduling policy for each slice	DRL-base, DRL-reduced-actions, DRL-no-autoencoder	Maximize rate for eMBB, PHY TBs for MTC, minimize buffer size for URLLC
sched	Multi-DRL-agent per-slice scheduling policy selection	Rate, buffer size, PRB ratio (DL)	Scheduling policy for each slice	DRL-sched	Maximize rate for eMBB and MTC, PRB ratio for URLLC
online-training	Train DRL agents with online exploration	Rate, buffer size, PHY TBs (DL)	Training action (PRB and scheduling)	Trained online by the xApp itself	Based on specific training goals

TABLE 1: Catalogue of developed xApps.

the agent (DRL-no-autoencoder). The `sched` xApp includes three DRL agents that select in parallel the scheduling policy for each slice (eMBB, MTC, and URLLC). Each agent has been trained using slice-specific data.

4.2 Training the DRL Agents

DRL agents are trained on the dataset described in Section 4.3, where at each training episode we select RAN data from different base stations to remove dependence on a specific wireless environment (Section 6) and facilitate generalization.

Following O-RAN specifications, training is performed offline on the dataset. In our case, this is achieved by randomly selecting instances in which the network reaches the state s_1 that results from the combination of the previous state s_0 and the action to explore a_0 .

In our experiments, the actor and critic networks of all DRL agents have been implemented as two fully-connected neural networks with 5 layers with 30 neurons each and an hyperbolic tangent activation function. The encoder consists of 4 fully-connected layers with 256, 128, 32 and 3 neurons and a rectified linear activation function. For all models, the learning rate is set to 0.001.

Finally, as illustrated in Table 1, we also consider the case of online training where the `online-training` xApp supports training a DRL agent using live data from the RAN and performing exploration steps on the online RAN infrastructure itself. While this is not recommended by O-RAN [5], it specializes the trained model to the specific deployment. We will discuss the tradeoffs involved in this operation in Section 6. `online-training` leverages TensorFlow CheckPoint objects to save and restore a (partially) trained model for multiple consecutive rounds of training. In this way, the training services in the xApp can restore an agent trained on an offline dataset using it as starting point for the online, live training on the RAN.

4.3 Large-scale Data Collection for CoO-RAN

To train the DRL agents for the CoO-RAN xApps we performed large-scale data collection experiments on Colosseum. The parameters for the scenario are summarized in Table 2.

The large-scale RF scenario mimics a real-world cellular deployment in downtown Rome, Italy, with the positions of the base stations derived from the OpenCellID database [26]. We instantiated a softwareized cellular network with 7 base stations through the SCOPE framework. Each base station

Parameter	Value
Number of nodes	$N_{BS} = 7, N_{UE} = 42$
RF parameters	DL carrier $f_d = 0.98$ GHz, UL carrier $f_u = 1.02$ GHz, bandwidth $B = 10$ MHz (50 PRBs)
Schedulers	RR, WF, PF
Slices	eMBB, MTC, URLLC (2 UEs/BS/slice)
Traffic profiles	Slice-based: 4 Mbit/s/UE for eMBB, 44.6 kbit/s/UE for MTC, 89.3 kbit/s/UE URLLC Uniform: 1.5 Mbit/s/UE for eMBB, MTC, URLLC

TABLE 2: Configuration parameters for the considered scenario.

operates on a 10 MHz channel (50 PRBs) which can be dynamically assigned to the 3 slices (i.e., eMBB, MTC, URLLC). Additionally, we considered two different TGEN traffic scenarios: slice-based traffic and uniform traffic. In slice-based traffic, users are distributed among different traffic profiles (4 Mbit/s constant bitrate traffic to eMBB users, and 44.6 kbit/s and 89.3 kbit/s Poisson traffic to MTC and URLLC, respectively). The uniform traffic is configured with 1.5 Mbit/s for all users. The training of the DRL agents on the offline dataset has been performed with slice-based traffic. Finally, the base stations serve a total of 42 users equally divided among the 3 slices.

In our data collection campaign, we gathered 3.4 GB of data, for a total of more than 73 hours of experiments. In each experiment, the base stations periodically report RAN KPMs to the non-real-time RIC. These include metrics such as throughput, buffer queues, number of PHY Transport Blocks (TBs) and PRBs. The complete dataset features more than 30 metrics that can be used for RAN analysis and ML training.

5 DRL-BASED XAPP EVALUATION

Learning strategies for RAN control are coded as xApps on CoO-RAN. This section presents their comparative performance evaluation. Feature selection based on RAN KPMs is described in Section 5.1. The experimental comparison of the different DRL models is reported in Section 5.2.

5.1 RAN KPM and Feature Selection

O-RAN is the first architecture to introduce a standardized way to extract telemetry and data from the RAN to drive closed-loop control. However, O-RAN does not indicate which KPMs should be considered for the design of ML

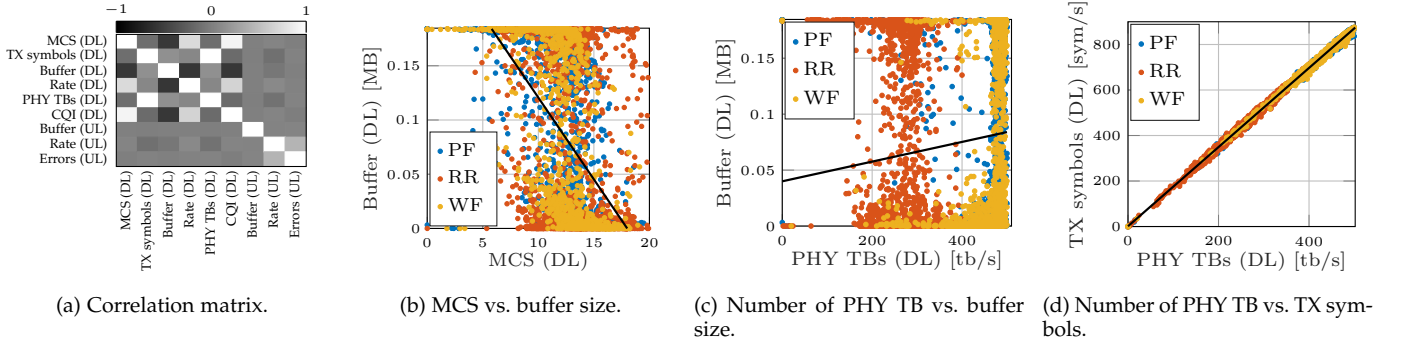


Fig. 4: Correlation analysis for the eMBB slice with 36 PRBs and the slice-based traffic profile. The solid line is the linear regression fit of the data.

algorithms. The O-RAN E2SM KPM specifications [15] allow the generation of more than 400 possible KPMs, listed in [27, 28]. More vendor-specific KPMs may also be reported on E2. These KPMs range from physical layer metrics to base station monitoring statistics. Therefore, the bulk set of data may not be useful to represent the network state for a specific problem. Additionally, reporting or collecting all the metrics via the E2 or O1 interfaces introduces a high overhead, and a highly dimensional input may lead to sub-optimal performance for ML-driven xApps [29].

Therefore, a key step in the design process of ML-driven xApps is the selection of the features that should be reported for RAN closed-loop control. In this context, the availability of large-scale, heterogeneous datasets and wireless data factories is key to enable feature selection based on a combined expert- and data-driven approach. To better illustrate this, in Fig. 4 and 5 we report a correlation analysis for several metrics collected in the dataset described in Section 4.3. The correlation analysis helps us identify the KPMs that provide a meaningful description of the network state with minimal redundancy.

Correlation analysis. Figure 4a shows the correlation matrix of 9 among the 30 UE-specific metrics in the dataset for the eMBB slice. While downlink and uplink metrics exhibit a low correlation, most downlink KPMs positively or negatively correlate with each other (the same holds for uplink KPMs). For example, the downlink Modulation and Coding Scheme (MCS) and buffer occupancy have a negative correlation (-0.56). This can also be seen in the

scatter plot of Fig. 4b: as the MCS increases, it is less likely to have a high buffer occupancy, and vice versa. Similarly, the number of TBs and symbols in downlink have a strong positive correlation (0.998), as also shown in Fig. 4d. Two downlink metrics that do not correlate well, instead, are the number of TBs and the buffer occupancy. Indeed, the amount of data transmitted in each TB varies with the MCS and therefore cannot be used as indicator of how much the buffer will empty after each transmission. Additionally, as shown in Fig. 4c, the three scheduling policies have a different quantitative behavior, but they all show a low correlation.

eMBB vs. URLLC. The correlation among metrics also depends on the RAN configuration and slice traffic profile. This can be seen by comparing Fig. 4, which analyzes the eMBB slice with 36 PRBs, and Fig. 5, which uses telemetry for the URLLC slice with 11 PRBs. With the slice-based traffic, the URLLC users receive data at a rate that is an order of magnitude smaller than that of the eMBB users. As a consequence, the load on the URLLC slice (represented by the buffer occupancy of Fig. 5b) is lower, and the buffer is quickly drained even with lower MCSs. Consequently, the correlation among the buffer occupancy and the MCS (-0.2) is lower with respect to the eMBB slice. This further makes the case for collecting datasets that are truly representative of a wireless RAN deployment, including heterogeneous traffic and diverse applications.

Summary. Figure 4 and 5 provide insights on which metrics can be used to describe the RAN status. Since the number of downlink symbols and TBs, or the MCS and the buffer occupancy for the eMBB slice are highly correlated, using them to represent the state of the network only increases the dimensionality of the state vector without introducing additional information. Conversely, the buffer occupancy and the number of TBs enrich the representation with low redundancy. Therefore, the DRL agents for the xApps in this paper consider as input metrics the number of TBs, the buffer occupancy (or the ratio of PRB granted and requested, which has a high correlation with the buffer status), and the downlink rate.

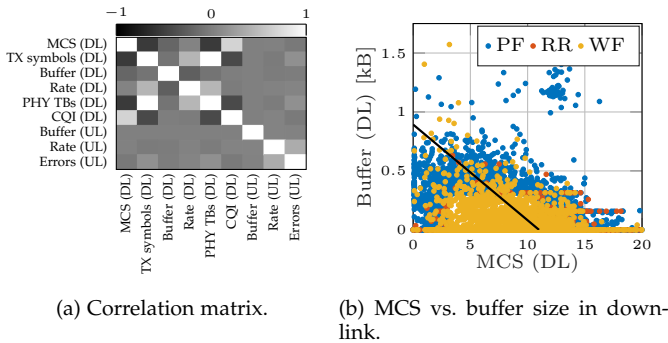
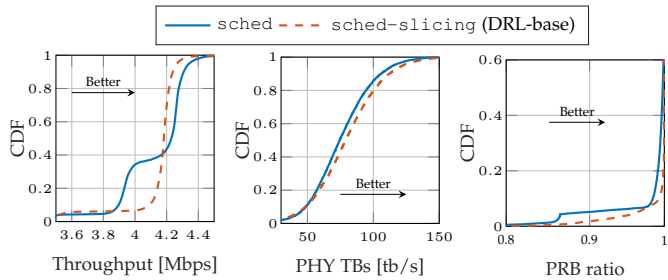


Fig. 5: Correlation analysis for the URLLC slice with 11 PRBs and the slice-based traffic profile. The solid line is the linear regression fit of the data.

5.2 Comparing Different DRL-based RAN Control Strategies

Once the input metrics have been selected, the next step in the design of ML applications involves the selection of the



(a) eMBB throughput. (b) MTC PHY TBs. (c) URLLC PRB ratio.

Fig. 6: Comparison between the `sched` and `sched-slicing` xApps, with the slice-based traffic profile. The slicing for the `sched` xApp is fixed and based on the configuration chosen with highest probability by the `sched-slicing` xApp (36 PRBs for eMBB, 3 for MTC, 11 for URLLC).

proper modeling strategy [5]. In this paper, we consider ML models for sequential decision making, and thus focus on DRL algorithms.

Control policy selection. In this context, it is clearly crucial to properly select the control knobs, i.e., the RAN parameters that need to be controlled and adapted automatically, and the action space, i.e., the support on which these parameters can change. To this end, Fig. 6 compares the performance for the `sched` and `sched-slicing` xApps, which perform different control actions. The first assumes a fixed slicing profile and includes three DRL agents that select the scheduling policy for each slice, while the second jointly controls the slicing (i.e., number of PRBs allocated to each slice) and scheduling policies with a single DRL agent. For this comparison, the slicing profile for the `sched` xApp evaluation matches the configuration that is chosen most often by the `sched-slicing` agent, and the source traffic is slice-based. The Cumulative Distribution Functions (CDFs) of Fig. 6 show that the joint control of slicing and scheduling improves the relevant metric for each slice, with the most significant improvements in the PRB ratio and in the throughput for the users below the 40th percentile. This shows that there exist edge cases in which adapting the slicing profile further improves the network performance with respect to adaptive schedulers with a static slice configuration, even if the fixed slicing configuration is the one that is chosen most often by the `sched-slicing` xApp.

DRL agent design. To further elaborate on the capabilities of `sched-slicing`, in Fig. 7 we compare results for different configurations of the DRL agent of the xApp, as well as for a static baseline without slicing or scheduling adaptation, using the slice-based traffic. The slicing profile for the static baseline is the one chosen most often by the `sched-slicing` xApp. The results of Fig. 7 further highlight the performance improvement introduced by adaptive, closed-loop control, with the DRL-driven control outperforming all baselines.

Additionally, this comparison spotlights the importance of careful selection of the action space for the DRL agents. By constraining or expanding the action space that the DRL agents can explore, the xApp designer can bias the selected policies. Consider the DRL-base and DRL-reduced-actions agents (see Table 1), whose difference is in the set of actions that the DRL agent can explore. Notably, the DRL-reduced-

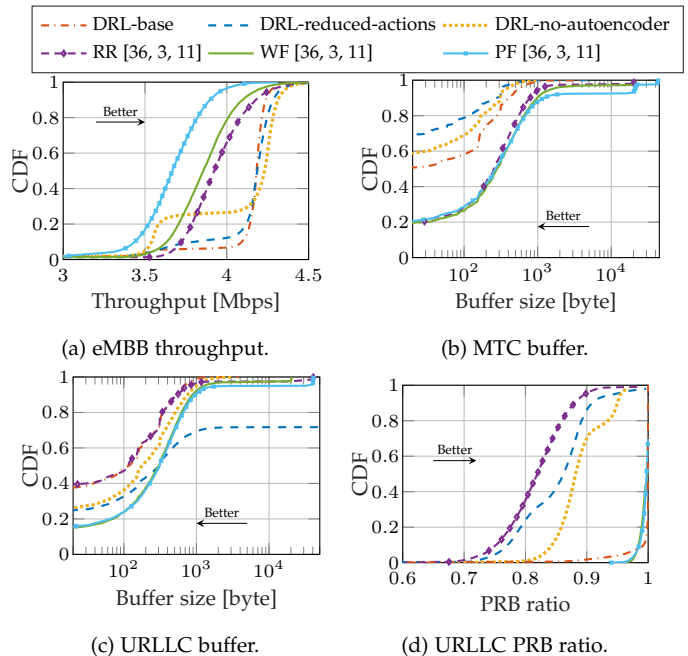


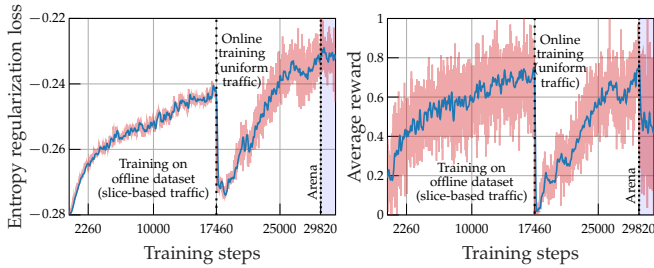
Fig. 7: Comparison between the `sched-slicing` xApp and baselines without DRL-based adaptation. For the latter, the performance is based on the slicing configuration chosen with highest probability by the best-performing DRL agent, and the three scheduler policies.

actions agent lacks the action that results in the policy chosen most often by the DRL-base agent. Compared to the most common action chosen by the DRL-reduced-actions agent (36 PRB for eMBB, 9 for MTC, 5 for URLLC), the most likely policy of DRL-base agent favors the URLLC over the MTC slice (11 vs. 3 PRBs). This is reflected in the performance metrics for the different slices. Notably, DRL-reduced-actions fails to maintain a small buffer and high PRB ratio for the URLLC slice (Fig. 7c and 7d), but achieves the smallest buffer occupancy for the MTC traffic.

Autoencoder. Finally, the results of Fig. 7 show the benefit of using an autoencoder, as the DRL-base and DRL-reduced-actions agents generally outperform the DRL-no-autoencoder agent. Indeed, the autoencoder decreases the dimensionality of the input for the DRL agent, improving the mapping between the network state and the actions. Specifically, the autoencoder used in this paper reduces a matrix of $T = 10$ input vectors with $N = 3$ metrics each to a single N -dimensional vector. Second, it improves the performance with online inference on real RAN data. Indeed, one of the issues of operating ML algorithms on live RAN telemetry is that some entries may be reported inconsistently or may be missing altogether. To address this, we train the autoencoder simulating the presence of a random number of zero entries in the training dataset. This allows the network to be able to meaningfully represent the state even if the input tensor is not fully populated with RAN data.

6 ONLINE TRAINING FOR DRL-DRIVEN XAPPS

The last set of results presents an analysis of the tradeoffs associated with training DRL agents on a live network



(a) Entropy regularization loss.

(b) Reward.

Fig. 8: Metrics for the training on the offline dataset and the online training on Colosseum and Arena. The Arena configuration uses LTE band 7. Notice that the Arena deployment considers 3 users per base station, contrary to the 6 users per base station of Colosseum, thus the absolute average reward decreases.

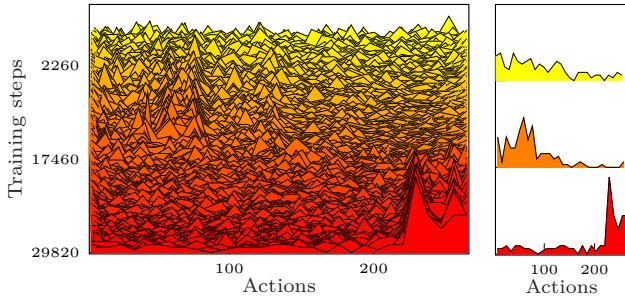


Fig. 9: Distribution of the actions during the training on the offline dataset and the online training on Colosseum. The offline training stops at step 17460.

in an online fashion. These include the evaluation of the time required for convergence, the impact of the exploration process on the RAN performance, and the benefits involved with this procedure. To do this, we load on the `online-training` xApp a model pre-trained on the offline dataset with the slice-based traffic profile. The same model is used in the DRL-reduced-actions agent. We deploy the `online-training` xApp on a CoLO-RAN base station and further continue the training with online exploration, using the uniform traffic profile (with the same constant bitrate traffic for each user). Additionally, we leverage the containerized nature of CoLO-RAN to deploy it on Arena [11], a publicly available indoor testbed, and perform training with one SDR base station and three smartphones.

Convergence. Figures 8 and 9 show how quickly the pre-trained agent adapts to the new environment. In particular, Fig. 8a reports the entropy regularization loss as a function of the training step of the agent. This metric correlates with the convergence of the training process: the smaller the absolute value of the entropy, the more likely the agent has converged to a set of actions that maximize the reward in the long run [30]. We stop the training when this metric (and the average reward, Fig. 8b) plateaus, i.e., at step 17460 for the offline training, step 29820 for the online training on Colosseum. The loss remains stable when transitioning from the Colosseum to the Arena online training, while it increases (in absolute value) when switching traffic profile at step 17460. This shows that the agent can better generalize across different channel conditions than source traffic profiles. The same trend can be observed in the average

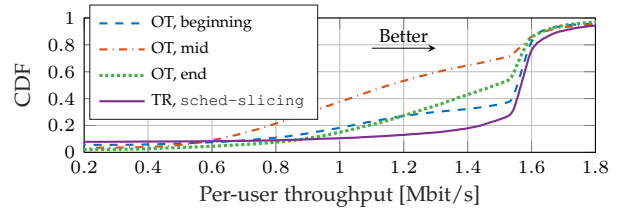


Fig. 10: CDF of the throughput for the eMBB slice during the online training (OT) and with the trained agent (TR) with the uniform traffic profile.

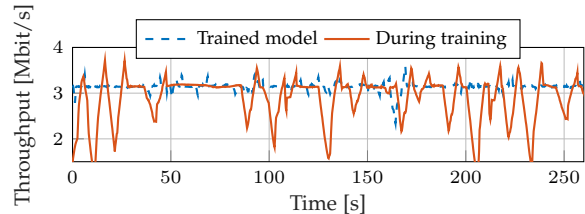


Fig. 11: eMBB slice throughput during training and with the trained model.

reward (Fig. 8b), with the difference that the transition from Colosseum to Arena halves the reward (as this configuration features 3 and not 6 users for each base station). While the Colosseum online training requires 30% fewer steps than the initial offline training, it also comes with a higher wall-clock time. Indeed, offline exploration allows the instantiation of multiple parallel learning environments. Because of this, the Colosseum DGX supports the simultaneous exploration of 45 network configurations. Instead, online training can explore one configuration at a time, leading to a higher wall-clock time.

Figure 9 reports the evolution of the distribution of the actions chosen by the DRL agent for the Colosseum offline and online training. Three histograms for steps 2260, 17460 (end of offline training) and 29820 (end of online training) are also highlighted in the plot on the right. During training, the distribution of the actions evolves from uniform (in yellow) to more skewed, multi-modal distributions at the end of the offline training (in orange) and online training (in red). Additionally, when the training on the new environment begins, the absolute value of the entropy regularization loss increases (Fig. 8a), and, correspondingly, the distribution starts to change, until convergence to a new set of actions is reached again.

Impact of online training on RAN performance. Achieving convergence with a limited number of steps is particularly important for online training, as the performance of the RAN may be negatively affected during the training process. Figure 10 reports the CDF for the user throughput during training and after, when the agent trained online is deployed on the `sched-slicing` xApp. The performance worsens when comparing the initial training step, which corresponds to the agent still using the actions learned during offline training, with an intermediate step, in which it is exploring random actions. Once the agent identifies the policies that maximize the reward in the new environment (in this case, with the uniform source traffic profile), the throughput improves. The best performance,

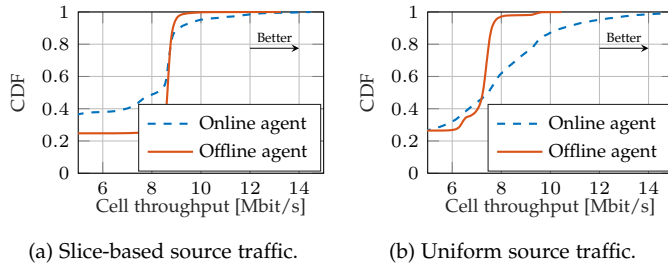


Fig. 12: Throughput comparison between the offline- and online-trained models with two source traffic patterns. The offline agent is the DRL-base for the `sched-slicing` xApp.

however, is achieved with the trained agent, which does not perform any exploration. Figure 11 further elaborates on this by showing how the online training process increases the throughput variability for the two eMBB users. Therefore, performing online training on a production RAN may be something a telecom operator cannot afford, as it may temporarily lead to disservices or reduced quality of service for the end users. In this sense, testbeds such as Colosseum can be an invaluable tool for two reasons. First, they provide the infrastructure to test pre-trained ML algorithms—and ColO-RAN enables any RAN developer to quickly onboard and test their xApps in a standardized O-RAN platform. Second, they allow online training without affecting the performance of production environments.

Adaptability. The main benefit of an online training phase is to allow the pre-trained agent to adapt to updates in the environment that are not part of the training dataset. In this case, the agent trained by the `online-training` xApp adapts to a new configuration in the slice traffic, i.e., the uniform traffic profile. Figure 12 compares the cell throughput for the agent before/after the online training, with the slice-based (Fig. 12a) and the uniform traffic (Fig. 12b). Notably, the online agent achieves a throughput comparable with that of the agent trained on the offline dataset with slice-based traffic, showing that—despite the additional training steps—it is still capable of selecting proper actions for this traffic profile. This can also be seen in Fig. 13, which shows that the action selected most often grants the most PRBs to the eMBB slice (whose users have a traffic one order of magnitude higher than MTC and URLLC).

The online agent, however, outperforms the offline-trained agent with the uniform traffic profile, with a gap of 2 Mbit/s in the 80th percentile, demonstrating the effectiveness of the online training to adapt to the updated traffic. The action profile also changes when comparing slice-based and uniform traffic, with a preference toward more balanced PRB allocations.

Summary. These results show how online training can help pre-trained models evolve and meet the demands of the specific environment in which they are deployed, at the cost, however, of reduced RAN performance during training. This makes the case for further research in this area, to develop, for example, smart scheduling algorithms that can alternate training and inference/control steps according to the needs of the network operator. Additionally, we showed that models pre-trained on Colosseum can be effective also in over-the-air deployments, making the case for ColO-RAN

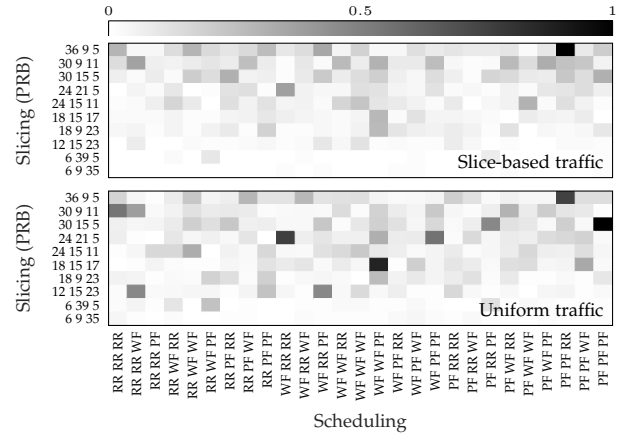


Fig. 13: Probability of selecting a slicing/scheduling combination for the online-trained agent with two different source traffic patterns. For each tuple, the first element refers to the PRB (scheduling) for the eMBB slice, the second for the MTC slice, and the third for the URLLC slice.

as a platform to train and test O-RAN ML solutions in a controlled environment.

7 RELATED WORK

The application of ML to wireless networks has received considerable attention in recent years. Existing works span the full protocol stack, with applications to channel modeling, PHY and MAC layers, ML-based routing and transport, and data-driven applications [31–33].

Several papers review the potential and challenges of ML for wireless networks, discussing open issues and potential solutions. Kibria et al. highlight different areas in which ML and big data analytics can be applied to wireless networks [33]. Sun et al. [34] and Gunduz et al. [35] review the key learning techniques that researchers have applied to wireless, together with open issues. Similarly, Chen et al. focus on artificial neural network algorithms [36]. Other reviews can be found in [16, 37]. While these papers present a clear overview of open problems associated with learning in wireless networks, and sometimes include some numerical evaluations [3, 38], they do not provide results based on an actual large-scale deployment, as this paper does, thus missing key insights on using real data, with imperfections, and on using closed-loop control on actual radios.

When it comes to cellular networks, ML has been applied throughout the 3GPP protocol stack. Perenda et al. automatically classify modulation and coding schemes [39]. Their approach is robust with respect to modulation parameters that are not part of the training set—a typical problem in wireless networks. Again, at the physical layer, Huang et al. investigate learning-based link adaptation schemes for the selection of the proper MCS for eMBB in case of preemptive puncturing for URLLC [40]. Others apply ML to 5G network management and KPM prediction [41–43]. These papers, however, do not close the loop through the experimental evaluation of the control action or classification accuracy on real testbeds and networks. Chuai et al. describe a large-scale, experimental evaluation on a production network, but the evaluation is limited to a single performance metric [44].

DRL has recently entered the spotlight as a promising enabler of self-adaptive RAN control. Nader et al. consider a multi-agent setup for centralized control in wireless networks, but not in the context of cellular networks [45]. Wang et al. use DRL to perform handover [46]. Other papers analyze the theoretical performance of DRL agents for medium access [47] and user association [48]. Mollahasani et al. evaluate actor-critic learning for scheduling [49], and Zhou et al. applies Q-learning to RAN slicing [8]. Chinchali et al. apply DRL to user scheduling at the base station level [50]. Differently from these papers, we analyze the performance of DRL agents with a closed loop, implementing the control actions on a software-defined testbed with an O-RAN compliant infrastructure to provide insights on how DRL agents impact a realistic cellular network environment. Finally, [6, 7] consider ML/DRL applications in O-RAN, but provide a limited evaluation of the RAN performance without specific insights and results on using ML.

8 CONCLUSIONS

The paper presents the first large-scale evaluation of ML-driven O-RAN xApps for managing and controlling a cellular network. To this purpose, we introduce CoO-RAN, the implementation of the O-RAN architecture in the Colosseum network emulator. CoO-RAN features a RAN E2 termination, a near-real-time RIC with three different xApps, and a non-real-time RIC for data storage and ML training. We pledge to publicly release CoO-RAN to enable O-RAN-based experiments in Colosseum together with the dataset collected for this work. We demonstrate the effectiveness of CoO-RAN through results from the large-scale comparative performance evaluation of the xApps running on CoO-RAN and discuss key lessons learned on DRL-based closed-loop control. In particular, we learned that (i) it is crucial to choose meaningful input features for the network state to avoid unnecessarily highly dimensional input for the DRL agent and that (ii) the action space for the DRL agent needs to be properly designed. Our comparison of different scheduling and slicing adaptation strategies shows that autoencoders can help to deal with unreliable real RAN data. Finally, we provide insights on the live training of DRL agents in Colosseum and Arena.

REFERENCES

- [1] Ericsson, "Ericsson mobility report," June 2021. [Online]. Available: <https://www.ericsson.com/en/mobility-report>
- [2] M. Giordani, M. Polese, M. Mezzavilla, S. Rangan, and M. Zorzi, "Toward 6G networks: Use cases and technologies," *IEEE Comm. Mag.*, vol. 58, no. 3, pp. 55–61, March 2020.
- [3] Z. Xiong et al., "Deep reinforcement learning for mobile 5G and beyond: Fundamentals, applications, and challenges," *IEEE Vehic. Tech. Mag.*, vol. 14, no. 2, pp. 44–52, June 2019.
- [4] L. Bonati, M. Polese, S. D'Oro, S. Basagni, and T. Melodia, "Open, programmable, and virtualized 5G networks: State-of-the-art and the road ahead," *Computer Networks*, vol. 182, pp. 1–28, December 2020.
- [5] O-RAN Working Group 2, "O-RAN AI/ML workflow description and requirements-v1.01," O-RAN.WG2.AI/ML-v01.01 Technical Specification, April 2020.
- [6] S. Niknam et al., "Intelligent O-RAN for beyond 5G and 6G wireless networks," *arXiv:2005.08374 [eess.SP]*, May 2020.
- [7] L. Bonati, S. D'Oro, M. Polese, S. Basagni, and T. Melodia, "Intelligence and Learning in O-RAN for Data-driven NextG Cellular

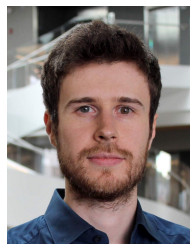
- Networks," *IEEE Communications Magazine*, vol. 59, no. 10, pp. 21–27, October 2021.
- [8] H. Zhou, M. Elsayed, and M. Erol-Kantarci, "RAN resource slicing in 5G using multi-agent correlated Q-learning," in *Proc. IEEE Intl. Symp. on Personal, Indoor and Mobile Radio Communications (PIMRC)*, Virtual Conference, September 2021.
- [9] L. Bonati, S. D'Oro, S. Basagni, and T. Melodia, "SCOPE: An open and softwarized prototyping platform for NextG systems," in *Proc. of ACM Intl. Conf. on Mobile Systems, Applications, and Services (MobiSys)*, Virtual Conference, June 2021.
- [10] L. Bonati et al., "Colosseum: Large-Scale Wireless Experimentation Through Hardware-in-the-Loop Network Emulation," in *Proc. of IEEE Intl. Symp. on Dynamic Spectrum Access Networks (DySPAN)*, Virtual Conference, December 2021.
- [11] L. Bertizzolo et al., "Arena: A 64-antenna SDR-based ceiling grid testing platform for sub-6 GHz 5G-and-beyond radio spectrum research," *Computer Networks*, vol. 181, pp. 1–17, November 2020.
- [12] O-RAN Working Group 1, "O-RAN Architecture Description - v2.00," O-RAN.WG1.O-RAN-Architecture-Description-v02.00 Technical Specification, July 2020.
- [13] S. D'Oro, L. Bonati, F. Restuccia, and T. Melodia, "Coordinated 5G Network Slicing: How Constructive Interference Can Boost Network Throughput," *IEEE/ACM Transactions on Networking*, vol. 29, no. 4, pp. 1881–1894, 2021.
- [14] O-RAN Alliance White Paper, "O-RAN use cases and deployment scenarios," <https://tinyurl.com/8cmtxmyy>, February 2020.
- [15] O-RAN Working Group 3, "O-RAN near-real-time RAN intelligent controller E2 service model (E2SM) KPM 1.0," ORAN-WG3.E2SM-KPM-v01.00.00 Technical Specification, February 2020.
- [16] J. Wang et al., "Thirty years of machine learning: The road to Pareto-optimal wireless networks," *IEEE Commun. Surveys Tuts.*, vol. 22, no. 3, pp. 1472–1514, Third quarter 2020.
- [17] U.S. Naval Research Laboratory, "MGEn Traffic Emulator." [Online]. Available: <https://tinyurl.com/beexe8yc>
- [18] O-RAN Software Community. Bronze release. <https://wiki.o-ran-sc.org/pages/viewpage.action?pageId=14221635>. Accessed July 2021.
- [19] I. Gomez-Miguel et al., "srsLTE: An open-source platform for LTE evolution and experimentation," in *Proc. of ACM Intl. Workshop on Wireless Network Testbeds, Experimental evaluation & Characterization (WiNTECH)*, New York City, NY, USA, October 2016.
- [20] O-RAN Software Community. O-DU-L2 Documentation. <https://docs.o-ran-sc.org/projects/o-ran-sc-o-du-l2/en/latest/index.html>. Accessed July 2021.
- [21] F. Capozzi, G. Piro, L. Grieco, G. Boggia, and P. Camarda, "Downlink Packet Scheduling in LTE Cellular Networks: Key Design Issues and a Survey," *IEEE Communications Surveys & Tutorials*, vol. 15, no. 2, pp. 678–700, Second 2013.
- [22] O-RAN Software Community. xApp Framework. <https://wiki.o-ran-sc.org/display/ORANSdk/xAppFramework>. Accessed July 2021.
- [23] M. Abadi et al., "TensorFlow: Large-scale machine learning on heterogeneous systems," 2015, software available from tensorflow.org. [Online]. Available: <https://www.tensorflow.org/>
- [24] S. Guadarrama et al., "TF-Agents: A library for reinforcement learning in TensorFlow," <https://github.com/tensorflow/agents>, 2018, [Online; accessed 25-June-2019]. [Online]. Available: <https://github.com/tensorflow/agents>
- [25] J. Schulman, F. Wolski, P. Dhariwal, A. Radford, and O. Klimov, "Proximal policy optimization algorithms," *arXiv:1707.06347 [cs.LG]*, July 2017.
- [26] Unwired Labs. OpenCellID. <https://opencellid.org>. Accessed July 2021.
- [27] 3GPP, "5G performance measurements," Technical Specification (TS) 28.552, June 2021, version 17.3.1.
- [28] —, "Performance measurements Evolved Universal Terrestrial Radio Access Network (E-UTRAN)," Technical Specification (TS) 32.425, June 2021, version 17.1.0.
- [29] M. Sakurada and T. Yairi, "Anomaly detection using autoencoders with nonlinear dimensionality reduction," in *Proc. of the 2nd Workshop on Machine Learning for Sensory Data Analysis*, ser. MLSDA'14, Gold Coast, Australia QLD, Australia, 2014, p. 4–11.
- [30] T. Haarnoja, H. Tang, P. Abbeel, and S. Levine, "Reinforcement learning with deep energy-based policies," in *Proc. of the 34th Intl. Conf. on Machine Learning*, ser. ICML'17, Sydney, NSW, Australia, 2017, p. 1352–1361.
- [31] T. J. O'Shea, K. Karra, and T. C. Clancy, "Learning to commu-

nicate: Channel auto-encoders, domain specific regularizers, and attention,” in *Proc. of IEEE Intl. Symp. on Signal Processing and Information Technology (ISSPIT)*, Limassol, Cyprus, Dec 2016, pp. 223–228.

- [32] S. Abbasloo, C.-Y. Yen, and H. J. Chao, “Wanna make your TCP scheme great for cellular networks? let machines do it for you!” *IEEE J. on Sel. Areas Commun.*, vol. 39, no. 1, pp. 265–279, January 2021.
- [33] M. G. Kibria *et al.*, “Big data analytics, machine learning, and artificial intelligence in next-generation wireless networks,” *IEEE Access*, vol. 6, pp. 32 328–32 338, 2018.
- [34] Y. Sun, M. Peng, Y. Zhou, Y. Huang, and S. Mao, “Application of machine learning in wireless networks: Key techniques and open issues,” *IEEE Commun. Surveys Tuts.*, vol. 21, no. 4, pp. 3072–3108, Fourth quarter 2019.
- [35] D. Gunduz *et al.*, “Machine learning in the air,” *IEEE J. Sel. Areas Commun.*, vol. 37, no. 10, pp. 2184–2199, October 2019.
- [36] M. Chen, U. Challita, W. Saad, C. Yin, and M. Debbah, “Artificial neural networks-based machine learning for wireless networks: A tutorial,” *IEEE Commun. Surveys Tuts.*, vol. 21, no. 4, pp. 3039–3071, Fourth quarter 2019.
- [37] C. Jiang *et al.*, “Machine learning paradigms for next-generation wireless networks,” *IEEE Wireless Commun.*, vol. 24, no. 2, pp. 98–105, April 2017.
- [38] Y. Fu, S. Wang, C.-X. Wang, X. Hong, and S. McLaughlin, “Artificial intelligence to manage network traffic of 5G wireless networks,” *IEEE Netw.*, vol. 32, no. 6, pp. 58–64, 2018.
- [39] E. Perenda, S. Rajendran, G. Bovet, S. Pollin, and M. Zheleva, “Learning the unknown: Improving modulation classification performance in unseen scenarios,” in *Proc. of IEEE INFOCOM 2021*, Virtual Conference, May 1–13 2021.
- [40] Y. Huang, T. Hou, and W. Lou, “A Deep-Learning-based Link Adaptation Design for eMBB/URLLC Multiplexing in 5G NR,” in *Proc. of IEEE INFOCOM 2021*, Virtual Conference, May 1–13 2021.
- [41] M. Polese *et al.*, “Machine learning at the edge: A data-driven architecture with applications to 5G cellular networks,” *IEEE Trans. Mob. Comput.*, pp. 1–16, June 2020.
- [42] D. Bega, M. Gramaglia, M. Fiore, A. Banchs, and X. Costa-Perez, “DeepCog: Cognitive network management in sliced 5G networks with deep learning,” in *Proc. of IEEE INFOCOM 2019*, Paris, France, April 29–May 2 2019, pp. 280–288.
- [43] J. Wang *et al.*, “Spatiotemporal modeling and prediction in cellular networks: A big data enabled deep learning approach,” in *Proc. of IEEE INFOCOM 2017*, Atlanta, GA, USA, May 2017, pp. 1–9.
- [44] J. Chuai *et al.*, “A collaborative learning based approach for parameter configuration of cellular networks,” in *Proc. of IEEE INFOCOM 2019*, Paris, France, April 29–May 2 2019, pp. 1396–1404.
- [45] N. Naderializadeh, J. J. Sydir, M. Simsek, and H. Nikopour, “Resource management in wireless networks via multi-agent deep reinforcement learning,” *IEEE Trans. Wireless Commun.*, vol. 20, no. 6, pp. 3507–3523, June 2021.
- [46] Z. Wang, L. Li, Y. Xu, H. Tian, and S. Cui, “Handover control in wireless systems via asynchronous multiuser deep reinforcement learning,” *IEEE Internet Things J.*, vol. 5, no. 6, pp. 4296–4307, December 2018.
- [47] S. Wang, H. Liu, P. H. Gomes, and B. Krishnamachari, “Deep reinforcement learning for dynamic multichannel access in wireless networks,” *IEEE Trans. Cogn. Commun. Netw.*, vol. 4, no. 2, pp. 257–265, June 2018.
- [48] N. Zhao *et al.*, “Deep reinforcement learning for user association and resource allocation in heterogeneous cellular networks,” *IEEE Trans. Wireless Commun.*, vol. 18, no. 11, pp. 5141–5152, Nov 2019.
- [49] S. Mollahasani, M. Erol-Kantarci, M. Hirab, H. Dehghan, and R. Wilson, “Actor-critic learning based QoS-aware scheduler for reconfigurable wireless networks,” *IEEE Trans. on Netw. Sci. Eng.*, pp. 1–10, 2021.
- [50] S. Chinchali *et al.*, “Cellular network traffic scheduling with deep reinforcement learning,” in *Proc. of Thirty-Second AAAI Conf. on Artificial Intelligence*, New Orleans, LA, 2018, pp. 766–774.



Michele Polese is an Associate Research Scientist at Northeastern University, Boston, since March 2020, working with Tommaso Melodia. He received his Ph.D. at the Department of Information Engineering of the University of Padova in 2020 under the supervision of with Michele Zorzi. He also was an adjunct professor and postdoctoral researcher in 2019/2020 at the University of Padova. During his Ph.D., he visited New York University (NYU), AT&T Labs in Bedminster, NJ, and Northeastern University, Boston, MA. He collaborated with several academic and industrial research partners, including Intel, InterDigital, NYU, AT&T Labs, University of Aalborg, King’s College and NIST. He was awarded with an Honorable Mention by the Human Inspired Technology Research Center (HIT) (2018), the Best Journal Paper Award of the IEEE ComSoc Technical Committee on Communications Systems Integration and Modeling (CSIM) 2019, and the Best Paper Award at WNS3 2019. His research interests are in the analysis and development of protocols and architectures for future generations of cellular networks (5G and beyond), in particular for millimeter-wave communication, and in the performance evaluation of complex networks. He is a Member of the IEEE.



Leonardo Bonati received his B.S. in Information Engineering and his M.S. in Telecommunication Engineering from University of Padova, Italy in 2014 and 2016, respectively. He is currently pursuing a Ph.D. degree in Computer Engineering at Northeastern University, MA, USA. His research interests focus on 5G and beyond cellular networks, network slicing, and software-defined networking for wireless networks.



Salvatore D’Oro received his Ph.D. degree from the University of Catania in 2015. He is currently a Research Assistant Professor at Northeastern University. He serves on the Technical Program Committee (TPC) of Elsevier Computer Communications journal and the IEEE Conference on Standards for Communications and Networking (CSCN) and European Wireless. He also served on the TPC of Med-Hoc-Net 2018 and several workshops in conjunction with IEEE INFOCOM and IEEE ICC. In 2015, 2016 and 2017 he organized the 1st, 2nd and 3rd Workshops on Competitive and COoperative Approaches for 5G networks (CO-COA). Dr. D’Oro is also a reviewer for major IEEE and ACM journals and conferences. Dr. D’Oro’s research interests include game-theory, optimization, learning and their applications to 5G networks. He is a Member of the IEEE.



Stefano Basagni is with the Institute for the Wireless Internet of Things and a professor at the ECE Department at Northeastern University, in Boston, MA. He holds a Ph.D. in electrical engineering from the University of Texas at Dallas (2001) and a Ph.D. in computer science from the University of Milano, Italy (1998). Dr. Basagni’s current interests concern research and implementation aspects of mobile networks and wireless communications systems, wireless sensor networking for IoT (underwater, aerial and terrestrial), and definition and performance evaluation of network protocols. Dr. Basagni has published over ten dozen of highly cited, refereed technical papers and book chapters. His h-index is currently 47 (December 2021). He is also co-editor of three books. Dr. Basagni served as a guest editor of multiple international ACM/IEEE, Wiley and Elsevier journals. He has been the TPC co-chair of international conferences. He is a distinguished scientist of the ACM, a senior member of the IEEE, and a member of CUR (Council for Undergraduate Education).



Tommaso Melodia is the William Lincoln Smith Chair Professor with the Department of Electrical and Computer Engineering at Northeastern University in Boston. He is also the Founding Director of the Institute for the Wireless Internet of Things and the Director of Research for the PAWR Project Office. He received his Ph.D. in Electrical and Computer Engineering from the Georgia Institute of Technology in 2007. He is a recipient of the National Science Foundation CAREER award. Prof. Melodia has served as

Associate Editor of IEEE Transactions on Wireless Communications, IEEE Transactions on Mobile Computing, Elsevier Computer Networks, among others. He has served as Technical Program Committee Chair for IEEE Infocom 2018, General Chair for IEEE SECON 2019, ACM Nanocom 2019, and ACM WUWnet 2014. Prof. Melodia is the Director of Research for the Platforms for Advanced Wireless Research (PAWR) Project Office, a \$100M public-private partnership to establish 4 city-scale platforms for wireless research to advance the US wireless ecosystem in years to come. Prof. Melodia's research on modeling, optimization, and experimental evaluation of Internet-of-Things and wireless networked systems has been funded by the National Science Foundation, the Air Force Research Laboratory the Office of Naval Research, DARPA, and the Army Research Laboratory. Prof. Melodia is a Fellow of the IEEE and a Senior Member of the ACM.